Biomaterials 35 (2014) 3919–3925

Contents lists available at ScienceDirect

Biomaterials

journal homepage: www.elsevier.com/locate/biomaterials

The relationship between glial cell mechanosensitivity and foreign body reactions in the central nervous system☆

Pouria Moshayedi [a,b,1,2], Gilbert Ng [a,2], Jessica C.F. Kwok [b], Giles S.H. Yeo [c], Clare E. Bryant [d], James W. Fawcett [b], Kristian Franze [a,e,*], Jochen Guck [a,f]

[a] Cavendish Laboratory, Physics Department, University of Cambridge, UK
[b] John van Geest Centre for Brain Repair, University of Cambridge, UK
[c] Metabolic Research Labs, Institute of Metabolic Science, University of Cambridge, UK
[d] Department of Veterinary Medicine, University of Cambridge, UK
[e] Department of Physiology, Development and Neuroscience, University of Cambridge, UK
[f] Biotechnology Center, Technische Universität Dresden, Dresden, Germany

ARTICLE INFO

Article history:
Received 1 November 2013
Accepted 15 January 2014
Available online 11 February 2014

Keywords:
Gliosis
Implant
FBR
Astrocyte
Microglia
Stiffness

ABSTRACT

Devices implanted into the body become encapsulated due to a foreign body reaction. In the central nervous system (CNS), this can lead to loss of functionality in electrodes used to treat disorders. Around CNS implants, glial cells are activated, undergo gliosis and ultimately encapsulate the electrodes. The primary cause of this reaction is unknown. Here we show that the mechanical mismatch between nervous tissue and electrodes activates glial cells. Both primary rat microglial cells and astrocytes responded to increasing the contact stiffness from physiological values ($G' \sim 100$ Pa) to shear moduli $G' \geq 10$ kPa by changes in morphology and upregulation of inflammatory genes and proteins. Upon implantation of composite foreign bodies into rat brains, foreign body reactions were significantly enhanced around their stiff portions *in vivo*. Our results indicate that CNS glial cells respond to mechanical cues, and suggest that adapting the surface stiffness of neural implants to that of nervous tissue could minimize adverse reactions and improve biocompatibility.

1. Introduction

Implantation of medical devices leads to a local foreign body reaction (FBR), which can cause local and systemic problems. In this process, implants are encapsulated by reactive tissue, which in the central nervous system (CNS) consists mainly of activated glial cells – microglia and astrocytes – surrounded by extracellular matrix. Glial cells make up about half of the cell population in the brain. Microglial cells are the resident immune cells of the CNS and the first line of defense, whereas astrocytes, which assume a multitude of functions, are the most abundant glial cells in the brain. The reactive process, which starts with the activation of glial cells, can damage local neurons, and the subsequent dendritic retraction and neuronal death may contribute to a gradual decline in the function of implanted electrodes [1–3].

Glial cell activation is characterized by hypertrophy (increase in volume and processes), proliferation (increase in cell number), and inflammatory reactions [4,5]. After subsidence of an acute injury response, implanted foreign bodies become chronically surrounded by activated microglial cells [6], which release proinflammatory and immunoregulatory substances [7], followed by a layer of reactive astrocytes [8] with an increased production of intermediate filaments (particularly glial fibrillary acidic protein, GFAP) [4,5]. The resulting glial scar may have a toxic effect on local neurons and acts as a physical barrier around the implant [6], thus insulating it from the remaining neurons and, in case of an electrode, detrimentally increasing its impedance [9].

The universal occurrence of the FBR is not well correlated with the chemical nature of the implant [10], which is generally selected to be inert. This poses the question about the trigger of an FBR. Importantly, CNS cells not only respond to chemical but also to mechanical signals (i.e., they are mechanosensitive). For example, most neuronal and glial cell types adapt their morphology and cytoskeletal composition to the stiffness of their surrounding *in vitro* [11–17].

* Corresponding author. Department of Physiology, Development and Neuroscience, University of Cambridge, Cambridge CB2 3DY, UK. Tel.: +44 1223 333761; fax: +44 1223 333840.
E-mail address: kf284@cam.ac.uk (K. Franze).
[1] Current address: Department of Neurology, University of California, LA, USA.
[2] These authors contributed equally to this work.

0142-9612/$ – see front matter © 2014 The Authors. Published by Elsevier Ltd. All rights reserved.
http://dx.doi.org/10.1016/j.biomaterials.2014.01.038

CNS tissue belongs to the softest tissues in nature [17], and neural implants are usually orders of magnitude stiffer than the physiological cell environment. Hence, it seemed possible that local cells respond to a mismatch of mechanical compliance between nervous tissue and the implant. To pursue this idea, we exposed microglia and astrocytes, the main contributors to FBRs in the CNS, to materials of different stiffness but same chemical properties and tested their morphological and inflammatory responses to these mechanical signals *in vitro* and *in vivo*.

2. Materials and methods

2.1. Cell cultures

Compliant culture substrates were fabricated from polyacrylamide as described previously [13] and functionalized with poly-D-lysine solution (PDL; Sigma) (see Supporting information for details and Fig. S5 for control measurements of rheological properties and PDL coating). All animal experiments were conducted in accordance with the United Kingdom Animals (Scientific Procedure) Act of 1986 and institutional guidelines. Cell cultures were prepared from neonatal Sprague–Dawley rat cerebral cortices as previously described [18]. 50,000 astrocytes or 100,000 microglia suspended in 300 μl culture medium were added onto each gel. All *in vitro* experiments were done after one day in culture.

2.2. Quantitative morphometry of glial cells

Phase contrast images of cells (72–344 cells per gel in 5–8 fields of view, 3 cultures per cell type) were taken. According to changes in morphology, four morphological categories were defined for microglia and five for astrocytes and arbitrary scores of 1 (for the round cell shape) to 4 or 5 (for the most spread cell shape) were assigned to each category [13] (Fig. 1).

2.3. Immunocytochemistry

Cells were fixed in 4% paraformaldehyde (PFA) for 10 min and washed in PBS three times for 10 min. Cells were then treated with 10% normal goat serum (Sigma) in PBS containing 0.1% Triton-X100 (Sigma; PBS-TX100) for 1 h. For IL-1β, the blocking step was performed with normal donkey serum (Stratech). Primary antibodies (or cocktails of primary antibodies; for details see Supporting information) were prepared in proper dilutions in PBS-TX100 and added to the cells. Cells were incubated for 2 h at room temperature, or alternatively overnight at 4 °C, washed, and incubated with appropriate secondary antibodies. After 1 h incubation at room temperature, cells were washed and mounted with FluorSave mounting reagent.

Image stacks were obtained with a confocal laser scanning microscope (Leica SP2 or Zeiss 510Meta). For Figs. 2 and 3, maximum projections were generated using ImageJ (NIH). In Fig. 2, gray levels were adjusted with Adobe Photoshop, settings for the same channels were kept constant for all samples.

2.4. Genome-wide profile of gene expression

Total RNA was extracted using RNeasy MinElute Cleanup Kit (QIAGEN) following the manufacturer's protocol. RNA quality and quantity was assessed using an RNA Pico Chip kit (RNA 6000 Pico Chip Kit, Agilent Technologies); genomic DNA was removed using the Ambion® TURBO DNA-*free*™ DNase Treatment (Ambion) kit. RNase activity was prohibited by implementing 20 Units of SUPERase-In (Ambion), and RNA quality and quantity evaluated again. Equal RNA quantities were processed with WT-Ovation™ Pico RNA Amplification System (NuGEN).

Sense-Target cDNA was generated, fragmented, biotinylated and hybridized onto Affymetrix Rat Gene 1.0 ST microarrays. The hybridized probe arrays were stained with streptavidin phycoerythrin conjugate and scanned using an Affymetrix GeneChip 7G scanner. Raw image data were converted to CEL using Affymetrix GeneChip Operating Software (GCOS). All downstream analysis of microarray data was performed using GeneSpring GX 11 (Agilent). CEL files were used for both the robust multiarray average (RMA) [19] and Probe Logarithmic Intensity Error estimation (PLIER) analyses [20], and expression values on the chip were normalized to the chip's 50th percentile. Each independent experiment included three arrays from three biological replicates. Statistical analysis was performed using a one-sample Student's *t*-test, which was applied to the mean of each normalized value against the baseline value of 1. Genes regulated differently by more than 1.3-fold from the control condition with a $P < 0.05$ were considered significant. Only genes which met the above criteria using RMA and PLIER were examined and shown in Tables S1, S2, S8 and S9.

Functional analyses were performed (Tables S3, S4, S10 and S11) using Ingenuity Pathway Analysis (IPA) (Ingenuity Systems Inc., USA; www.ingenuity.com) to identify the biological functions and diseases that were most significant to the data set (Tables S5, S6, S12 and S13). The significance of the association between the data set and the pathway was measured by two means: (1) A ratio of the number of molecules from the data set that map to the pathway divided by the total number of molecules that map to the canonical pathway is displayed and (2) Fisher's exact test was used to calculate a *P* value to determine the probability that the association between the genes in the data set and the pathway is due to chance

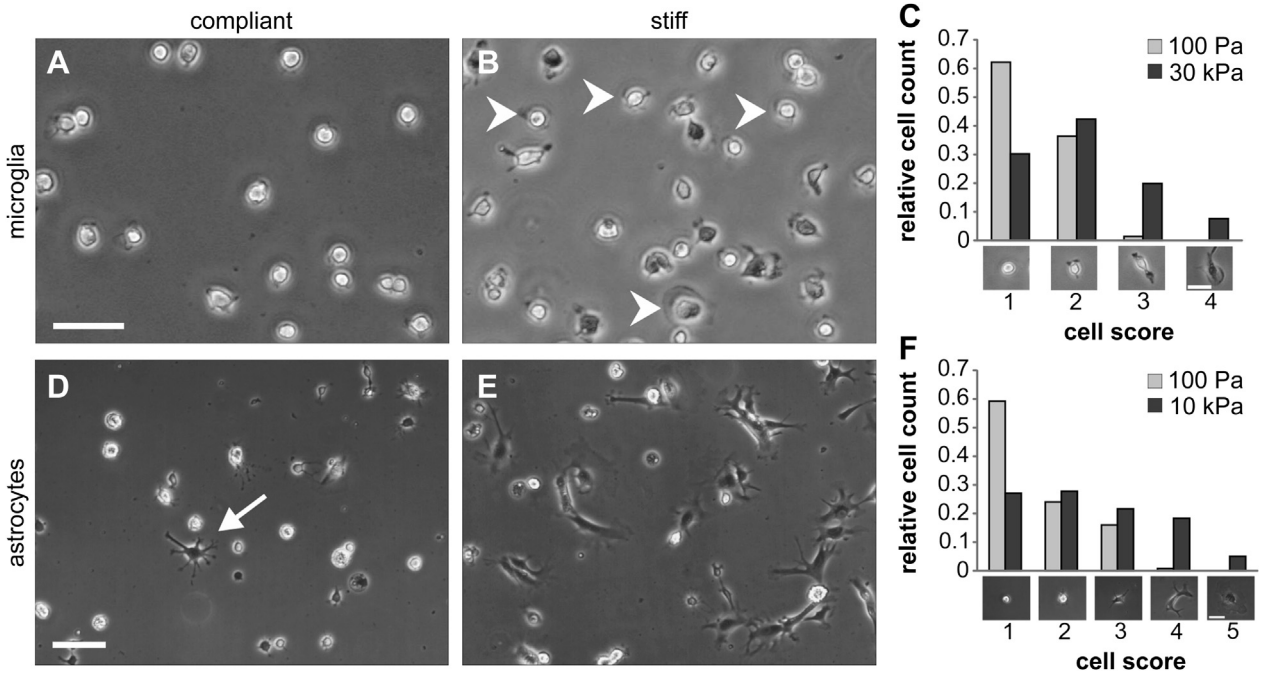

Fig. 1. Glial cell morphology depends on substrate stiffness. Both primary microglial cells (A–C) and astrocytes (D–F) change their morphology in response to the stiffness of the substrate. (A, D) On compliant substrates mimicking brain tissue elasticity ($G' = 100$ Pa) both cell types showed spherical morphologies. Moreover, astrocytes occasionally showed star-like morphologies, resembling their *in vivo* shape (arrow in D). (B, E) On stiffer substrates ($G' = 30$ kPa and 10 kPa for microglia and astrocytes, respectively), glial cells spread significantly more and extended several processes. An activated phenotype was frequently observed on stiff gels (arrowheads in B). Scale bars: 50 μm. (C, F) A quantitative cell shape analysis (score according to cell morphology [13]) confirmed that morphological changes in microglia and astrocytes cultured on stiff substrates were significant ($P_{microglia}$ = 1E-30 ($N_{stiff} = 447$; $N_{soft} = 418$); $P_{astrocytes}$ = 2E-39 ($N_{stiff} = 550$; $N_{soft} = 625$); Mann–Whitney test). Scale bars: 30 μm.

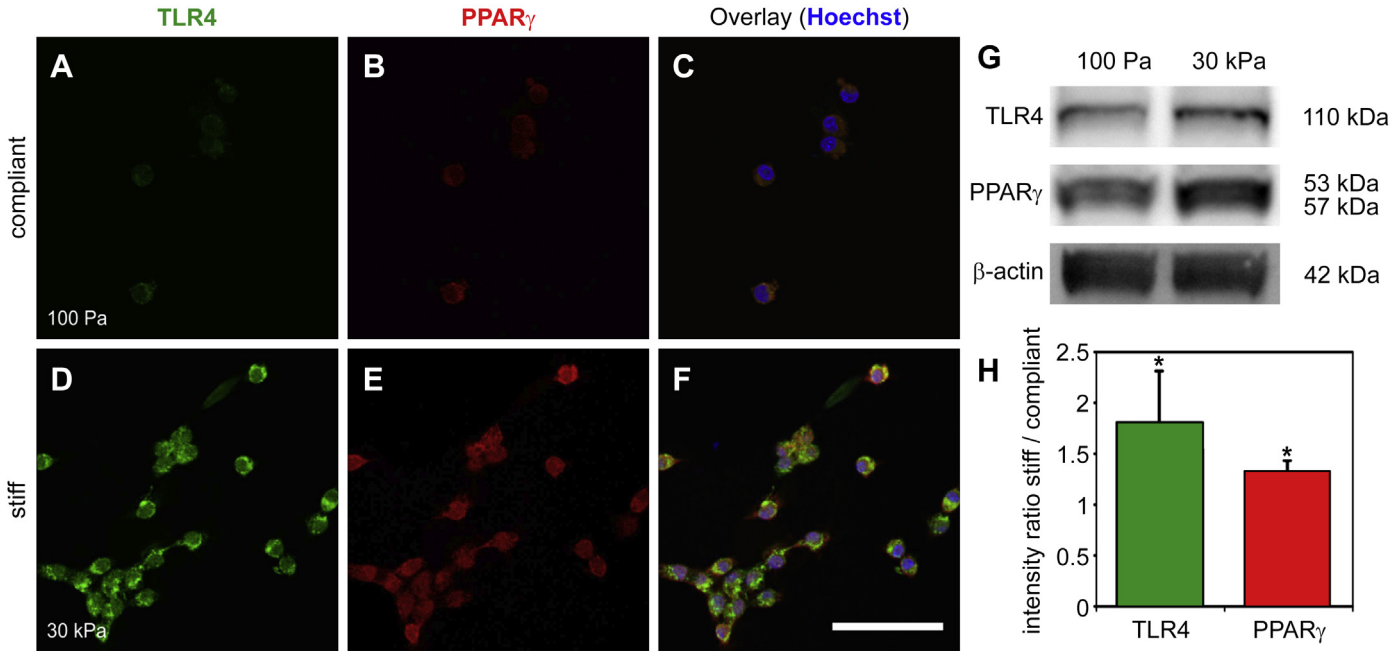

Fig. 2. Inflammatory responses of microglial cells to stiff substrates. (A–F) Fluorescence images of microglia cultured on compliant (A–C) and stiff (D–F) substrates for 1 day and stained for inflammatory mediators TLR4 (A, D) and PPARγ (B, E). (C, F) Overlay of PPARγ, TLR4, and Hoechst-labeled cell nuclei. Scale bar: 50 μm. (G) Western blots showing intracellular protein concentrations after 1 day in culture. (H) Quantitative analysis of Western blots revealed that both PPARγ and TLR4 levels were significantly upregulated on stiffer substrates ($N = 3$, $P < 0.05$, paired two-tailed t-test; mean ± S.E.M.).

alone. Functional analyses were performed on lists generated using only the PLIER algorithm.

2.5. Quantitative real-time PCR (qPCR)

A TaqMan real-time PCR method was applied to confirm changes in expression profiles of a selection of genes in microglia (i.e., LPL, RELA, PPARG, ALCAM, CCR1, CD9, CD97, CSF2, CSF3, P2RY1, TLR4, SDC4, ANGPT1 and TREM1). A separate set of RNA was extracted from microglia, purified and converted to cDNA as described above. Real-time PCR was run using TaqMan primers and reagents (Applied Biosystems) and arbitrary units of gene quantities were extracted from Ct values using the standard curves. Among BACTIN, GAPDH and B2M, BACTIN showed the smallest variation and was therefore selected as the house-keeping control.

2.6. Western blot analysis

Astrocytes were gently detached using ice-cold EDTA (5 mM in PBS, Sigma), spun down, resuspended in ice-cold PBS and pelleted again. Astrocytes were lysed using

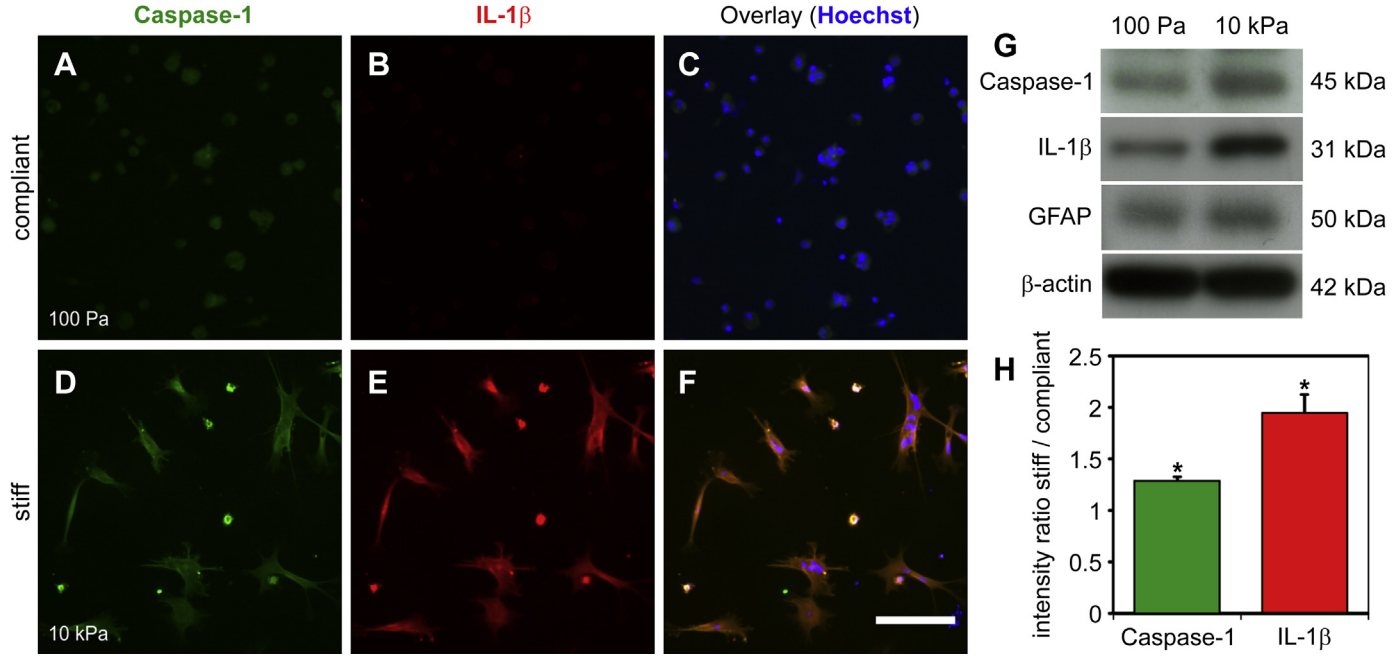

Fig. 3. Inflammatory response of astrocytes to stiff substrates. (A–F) Fluorescence images of astrocytes cultured on compliant (A–C) and stiff (D–F) substrates for 1 day and stained for inflammatory mediators Caspase-1 (A, D) and Interleukin 1β (B, E). (C, F) Overlay of Caspase-1, Interleukin 1β, and Hoechst-labeled cell nuclei. Scale bar: 100 μm. (G) Western blots showing intracellular protein concentrations after 1 day in culture. (H) Quantitative analysis of Western blots revealed that both pro-Caspase-1 and pro-Interleukin 1β levels were significantly upregulated on stiffer substrates ($N = 3$, $P < 0.05$; paired two-tailed t-test; mean ± S.E.M.).

Complete Lysis-M kit (Roche) at room temperature and extracted proteins were mixed with Laemmli sample buffer and incubated for 2 min at 95 °C. Microglia were collected similarly and equalized to ~2.25 × 10^6 cells. Cells were pelleted and lysed with 30 μl of ice-cold lysis buffer (Cell Signaling) supplemented with additional protease inhibitors (Complete Lysis-M kit, Roche) for 30–60 min. Intermittent vortexing and sonication was performed every 15 min. Laemmli sample buffer (Biorad) was added to cell lysates and heated to 100 °C for 10 min.

Samples were run through 4–20% gradient PAA gels (110V, Pierce) and transferred to 0.45 μm pore size polyvinylidene fluoride (PVDF) membranes (Fisher Scientific). Membranes were blocked in 5% skimmed milk dissolved in Tris buffered saline-Tween 20 (TBS-T; 20 mM Tris Base, 150 mM NaCl, and 0.1% Tween-20, Sigma) or 5% bovine serum albumin (BSA) for 60 min. Membranes were blotted for proteins (antibodies were dissolved in TBS-T containing 1% semi-skimmed milk) followed by horseradish peroxidase (HRP)-tagged secondary antibody treatment. Immunolabeled protein bands were visualized by chemiluminescence (ECL Plus, Amersham) on conventional X-ray film (Kodak). In microglial samples, avidin-biotin amplification (Vectastain, Vector labs) was used. Blots were visualized by CCD camera and UVISoft software (UVITEC Cambridge).

Western blots were quantified using ImageJ software. Briefly, images were inverted, boxes of equal size were drawn around the bands of interest, and mean white values (MWV) measured; background was measured accordingly and subtracted from the band values. The method was confirmed by Gaussian fitting analysis using Origin. Briefly, plot profiles of inverted blots were plotted and fitted to a Gaussian. Background was subtracted from the base of the curve and the integrated value of the curve was determined.

2.7. In vivo study

PAA premixes of 30 kPa and 100 Pa gels were polymerized on top of each other in a 0.2 ml PCR tube, removed, and treated as before. Cylindrical composite gels of ~3 mm length were prepared and implanted into brains of 14 Sprague–Dawley rats. After opening the skull, a composite foreign body was inserted into brain tissue using fine tweezers (Fig. 4). The insertion point was located 1.5 mm lateral to the midline mid-way between Bregma and Lambda planes. The brain was covered with the excised bony slab and the skin was sutured. Animals received analgesic injections for the following 2–3 days. 1 or 3 weeks after gel implantation, animals were overdosed with Euthanal (Merial Animal Health Ltd) and perfused transcardially using PBS followed by 4% PFA. Regions of interest were trimmed from the brains, post-fixed for 2 h in 4% PFA, immersed in a 25% sucrose solution overnight, cut along the coronal plane into 16 μm-thick slices using a Leica Cryostat (CM3000, Leica), and slices stained using immunohistochemistry (see Supporting information).

Images were taken using a confocal laser scanning microscope and stitched together using Corel Draw X3 software. The interface between the brain tissue and different gel types was determined using bright field images (Fig. S1). Fluorescence images were analyzed using Adobe Photoshop CS5 software. To capture local responses to foreign body stiffness, the edges of the lesion around the stiff and soft gels were separately found using the magic lasso tool, the border of the mask was extended to 50 pixels, and average gray values of these selections determined. This way, protein levels around the stiff and soft parts of the implant in the same animal were normalized for the contact area of implant and tissue (Fig. 4).

2.8. Statistical analysis

In vitro data was collected in all cases from at least three different cultures. Origin software (Version 8; OriginLab) was used to analyze the statistical significance of the data. Kolmogorov–Smirnov tests confirmed a normal distribution of values before any parametric test was employed.

3. Results

3.1. Cell morphology

In order to examine the putative effect of contact compliance on glial cells, we cultured primary rat microglia and astrocytes on polyacrylamide substrates of different compliance but identical poly-D-lysine surface coating [13] (Fig. 1). Two compliance regimes were used: shear storage moduli $G' = 100$ Pa, resembling physiological brain tissue elasticity [21,22], and 10 or 30 kPa, which is significantly stiffer than brain tissue and at least an order of magnitude above the substrate stiffness at which astrocytes undergo a transition from a compliant to stiff phenotype [13]. We studied morphological, gene and protein expression changes as a function of substrate stiffness after one day in culture.

Microglial cells growing on 100 Pa surfaces mostly showed spherical morphologies, with some short processes and lamellipodia (Fig. 1A). On stiff substrates ($G' = 30$ kPa) microglia spread more and assumed cell shapes generally seen in cultures on rigid surfaces (Fig. 1B) [23]. A quantitative analysis [13] showed significant morphological differences (Fig. 1C). Consistent with previous studies [12,13], astrocytes on compliant gels either had a rounded shape or a star-like morphology with fine processes, quite unlike their usual *in vitro* appearance on rigid substrates, but resembling their *in vivo* morphology (Fig. 1D). Astrocytes on stiff substrates ($G' = 10$ kPa) spread significantly more and acquired a polygonal shape as on rigid tissue culture plastic or glass surfaces (Fig. 1E). Quantitative shape analysis confirmed that also differences in astrocyte morphologies were significant (Fig. 1F). Hence, both microglia and astrocytes displayed morphological characteristics of an activated phenotype on stiffer substrates.

3.2. Gene and protein expression in microglia

We then investigated whether glial responses to mechanical stiffness might also involve the production of molecules that could trigger an inflammatory reaction. We first analyzed the transcriptional profile of microglial cells and astrocytes as a function of substrate compliance using DNA microarrays.

In microglial cells 73 genes were significantly upregulated on stiff substrates compared to compliant ones (Table S1) and 123 genes downregulated (Table S2). A functional gene expression analysis revealed, amongst others, significant increases in the inflammatory response ($P = 1.9E-06$), immune cell trafficking ($P = 9.6E-05$), cellular growth and proliferation ($P = 7.5E-05$), cell-mediated immune response ($P = 2.2E-04$), and antigen presentation ($P = 1.1E-04$) of microglia grown on stiff substrates (Table S3, for significant decreases see Table S4). In total, 15 pathways related to different inflammatory and pathogenic functions were upregulated on stiff substrates (Table S5), and 8 were attenuated (Table S6). Individual inflammation-related genes that were significantly enhanced in microglia cultured on the stiffer gels and that are important for FBR include markers of microglia activation (CD97 and PPARγ), receptors mediating microglia activation (TLR4 and TREM1), and receptors involved in adhesion and migration (CD9 and CD97). The increased expression of these genes was verified by qPCR (Table S7); immunocytochemistry and Western blots confirmed significant upregulation of PPARγ and TLR4 at the protein level (Fig. 2).

3.3. Gene and protein expression in astrocytes

Comparing gene expression in astrocytes that were grown on stiff substrates ($G' = 10$ kPa) relative to compliant substrates, we found a significant increase in the expression of 151 genes (Table S8) and a decrease of 57 genes (Table S9). A functional analysis of astrocytes grown on stiff substrates showed, amongst others, significant increases in their inflammatory response ($P = 1.5E-02$), cell-mediated immune response ($P = 2.6E-03$), cellular growth and proliferation ($P = 5.1E-03$), cell morphology ($P = 5.8E-03$), and cell-to-cell signaling and interaction ($P = 7.7E-03$) (Table S10; for significant decreases see Table S11). Individual genes that were enhanced on the stiffer substrates include inflammatory proteins (CASP1), microtubule organizers (TUBE1, MID1), molecular motors (KIF18B), extracellular matrix proteins (FBN1, CSGALNACT1, HYAL3), cell–cell adhesion proteins (PCDHGB6), and growth and differentiation proteins (CCNF, SMAD9, SEMA4C). In order to confirm these mRNA changes, we selected some key inflammation-related molecules, for which antibodies exist, for examination at the protein level by immunocytochemistry and Western blot. Astrocytes growing on stiff substrates contained significantly higher levels of pro-caspase-1

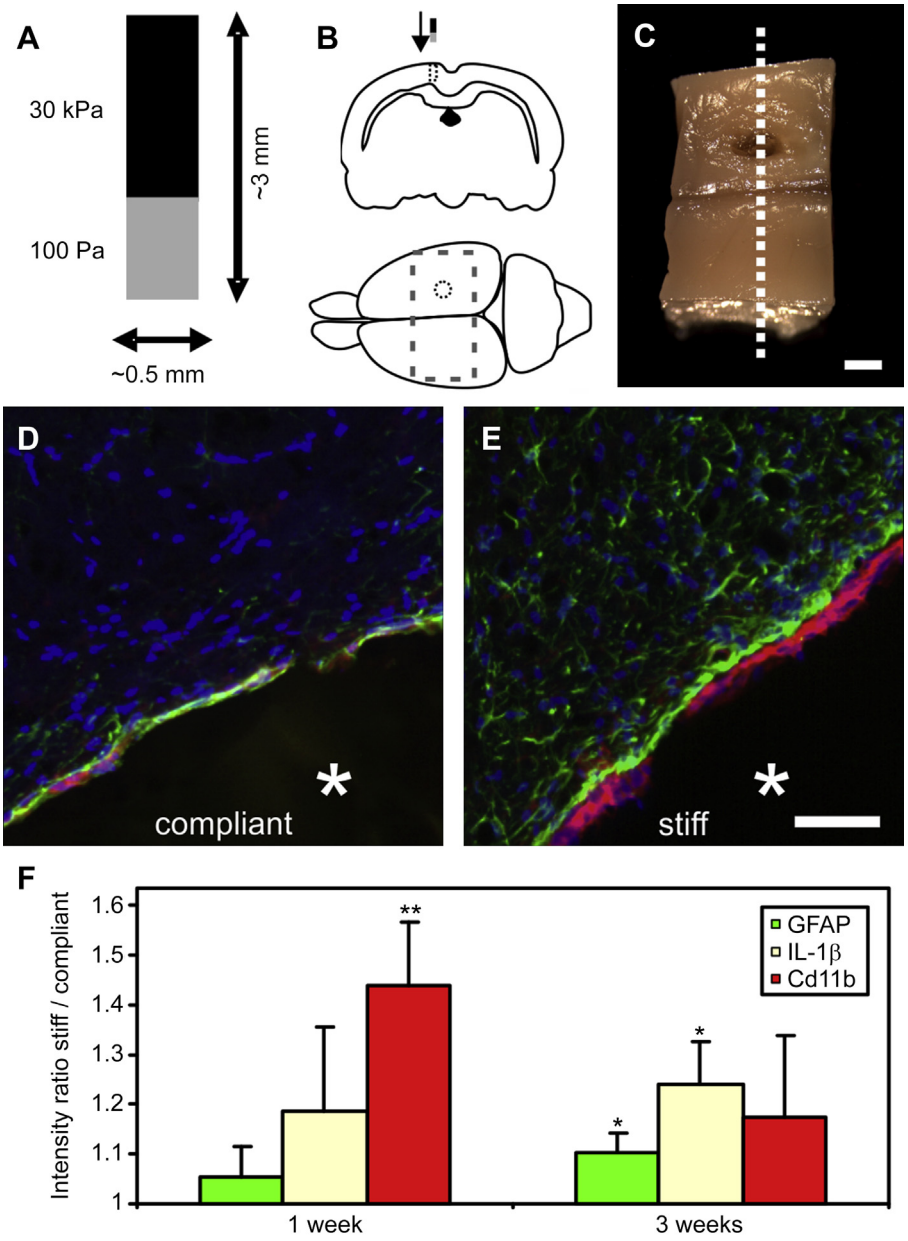

Fig. 4. ***In vivo*** **FBR is triggered by the stiffness of an implant**. (A) Schematic drawing of a composite foreign body (cFB) consisting of a compliant ($G' = 100$ Pa) and a stiff part ($G' = 30$ kPa), both made from polyacrylamide. (B) Schematic coronal section and top view of a rat brain indicating the location of the cFB (dotted lines). The dashed gray line indicates the region visible in (C), which shows brain tissue at the end of an experiment. Scale bar: 1 mm. (D) Immunohistochemistry of brain tissue in the vicinity of the compliant and (E) stiff part of a cFB (asterisks) implanted for three weeks; blue: Hoechst stained nuclei, red: CD11b (OX 42) showing activated microglial cells, green: GFAP showing activated astrocytes. Inflammatory and astrogliotic reactions are considerably increased around the stiff material (cf. Figs. S2, S3). Scale bar: 50 μm (F) A quantitative analysis of the fluorescence intensity of the brain tissue surrounding the cFB revealed that after one week the CD11b signal was significantly increased around its stiff portion ($P < 0.01$; $N = 5$; paired one-tailed *t*-test; mean ± S.E.M.), suggesting that more activated microglia were attracted towards the stiffer implant in the acute phase of the FBR. After three weeks, i.e., in the chronic phase, GFAP as well as Interleukin 1β expression were also significantly enhanced around the stiff part of the cFB ($P < 0.05$, $N = 5$ and 3, respectively), indicating that mechanical cues are involved in triggering gliotic and inflammatory reactions around foreign bodies, culminating in FBRs.

and pro-interleukin-1β (IL-1β) proteins (Fig. 3). IL-1β is considered to be at the top of the hierarchy of the neuroinflammatory mediator cascade [24].

3.4. In vivo experiments

The preceding results suggested that both astrocytes and microglial cells change gene and protein expression as well as morphology when grown on stiff materials compared to surfaces with a compliance equivalent to that of brain tissue. These changes on stiff substrates were characteristic of those seen in reactive gliosis and FBR. We therefore devised an *in vivo* test and implanted composite foreign bodies into rat brains to see whether gliosis and the accompanying FBR can be triggered by mechanical cues. These foreign bodies consisted of a compliant ($G' = 100$ Pa) and a stiff part ($G' = 30$ kPa) made from the same material (polyacrylamide) as used for the culture experiments. The grafts were left in place for one or three weeks. We then performed immunohistochemistry on

sections of the tissue surrounding the implant, observing markers of gliosis and inflammation (Fig. 4, S1–S3).

At one week, increased fluorescence of CD11b (OX 42) revealed a significant increase in microglial activation around the stiff portion of the foreign body if compared to its compliant region ($P = 0.008$, paired one-tailed *t*-test). GFAP levels in astrocytes were not significantly different in both regions ($P = 0.45$). After three weeks, however, reactive astrocytes surrounded the foreign body, with significantly higher GFAP levels around the stiff part of the implant ($P = 0.02$). Furthermore, IL-1β was significantly upregulated in the tissue in contact with the stiff part of the implants at that time point ($P = 0.04$) (Fig. 4E–G). Overall, three weeks after implantation cells organized into a dense and distinct layer of tissue that encircled the stiff portion of the implanted object.

4. Discussion

Our experiments show that both microglial cells and astrocytes, the key contributors to FBR in CNS tissue, respond to mechanical cues *in vitro* as well as *in vivo* in a way that is consistent with a mechanical trigger of FBR. Contact with an unphysiologically stiff surface causes both microglia and astrocytes to display an acute and late chronic inflammatory response typical for reactive gliosis. It is possible that glial reactions to mechanical cues and/or distributions of other cells which may contribute to glial scarring, such as pericytes [25], are cortical layer-specific. However, when comparing intensities of fluorescent inflammation and astrogliosis markers locally, and focusing on the tissue region where the soft and stiff parts of the implant met, we found very similar differences as in the global analysis shown in Fig. 4, indicating that our results are independent of the location within the cortex. Overall, our data suggest a significant contribution of glial cell mechanosensitivity to triggering gliosis and FBR around implants in the CNS.

The stiffness of different tissues in our body spans several orders of magnitude, from that of fat and brain tissue to that of bone and teeth. Most if not all animal tissue cells, including glial cells and neurons, are mechanosensitive and respond to mechanical stimuli in their environment. Deviations from the physiological mechanical properties of a tissue may accompany or even precede and/or contribute to pathological changes [26–28]. It is important to note that each type of tissue cell seems to have its own internal gauge for a 'normal' stiffness; cells from stiffer tissues usually experience larger stiffnesses as 'normal'. Our current study promotes the thesis that glial cells in the brain feel and respond to changes in the stiffness of their environment and react by isolating the "foreign", stiff object from the surrounding physiologically soft tissue.

Cellular mechanosensitivity is increasingly recognized as an important player in cell physiology and pathology. For example, stem cell differentiation can be directed by mechanical cues [29], towing by migrating cells can mechanically guide neuronal axon pathfinding *in vivo* [30], and mechanical forces can even act as second messenger in signal transduction [31]. While our data present direct proof for an involvement of mechanical signaling at the onset and during progression of FBR in the CNS, the molecular pathways leading to the mechano-responsiveness of glial cells remain elusive [17]. Our experiments reveal changes in the expression of many genes in glial cells grown on stiff substrates (Tables S1, S8), which could potentially be involved in their mechanosensitive response to foreign bodies [14,17]. Further work will investigate molecular mechanisms of glial cell mechanosensitivity.

5. Conclusions

FBR is a general phenomenon also found in other organ systems. It is likely that macrophages as the first line of defense in these organs will show similar responses to mechanical cues as do microglia in the nervous system [32]. Hence, our data suggest that adapting the surface mechanical properties of implants to the physiological stiffness of the organ in which they are embedded could significantly alleviate FBR. Since most cell types probe their substrate only a few tens of microns deep [33,34], a compliant coating of appropriate thickness might be sufficient to increase the life time of electrodes implanted into brain tissue, and alleviate FBR around other types of medical implants by improving their biocompatibility. This improved implant design aspect could significantly improve the quality of life of many patients that depend on long-term implant survival.

Acknowledgments

The authors would like to thank Stéphanie Lacour, Ivan Minev, Krystyn Van Vliet, Robin Franklin, and Kate Hughes for inspiring discussions and technical help. We would like to acknowledge financial support from the Cambridge Overseas Trust (ORS equivalent bursary to PM), the UK Engineering and Physical Sciences Research Council (Basic Technology Grant to PM, JWF, KF, JG), the European Union FP7 programs EurOCHIP, Full4Health (GSHY), and Angioscaff (JCFK), the MRC Centre for Obesity and Related Metabolic Disorders (GSHY), the UK Biotechnology and Biological Sciences Research Council (Research Development Fellowship to CEB), the Christopher and Dana Reeves Foundation (JWF), the Human Frontier Science Program (JG), the Marie Curie Initial Training Network "Transpol" (GN, JG), the Alexander von Humboldt Foundation (Feodor Lynen Fellowship to KF, AvH Professorship to JG), and the UK Medical Research Council (Career Development Award to KF).

Appendix A. Supplementary data

Supplementary data related to this article can be found at http://dx.doi.org/10.1016/j.biomaterials.2014.01.038.

References

[1] Polikov VS, Tresco PA, Reichert WM. Response of brain tissue to chronically implanted neural electrodes. J Neurosci Methods 2005;148:1–18.
[2] Grill WM, Norman SE, Bellamkonda RV. Implanted neural interfaces: biochallenges and engineered solutions. Annu Rev Biomed Eng 2009;11:1–24.
[3] Tresco PA, Winslow BD. The challenge of integrating devices into the central nervous system. Crit Rev Biomed Eng 2011;39:29–44.
[4] Silver J, Miller JH. Regeneration beyond the glial scar. Nat Rev Neurosci 2004;5:146–56.
[5] Pekny M, Nilsson M. Astrocyte activation and reactive gliosis. Glia 2005;50:427–34.
[6] He W, Bellamkonda RV. A molecular perspective on understanding and modulating the performance of chronic central nervous system (CNS) recording electrodes. In: Reichert WM, editor. Indwelling neural implants: strategies for contending with the in vivo environment. Boca Raton (FL): CRC Press; 2008.
[7] Kettenmann H, Hanisch UK, Noda M, Verkhratsky A. Physiology of microglia. Physiol Rev 2011;91:461–553.
[8] Popovich PG, Wei P, Stokes BT. Cellular inflammatory response after spinal cord injury in Sprague–Dawley and Lewis rats. J Comp Neurol 1997;377:443–64.
[9] He W, McConnell GC, Bellamkonda RV. Nanoscale laminin coating modulates cortical scarring response around implanted silicon microelectrode arrays. J Neural Eng 2006;3:316–26.
[10] Bryers JD, Giachelli CM, Ratner BD. Engineering biomaterials to integrate and heal: the biocompatibility paradigm shifts. Biotechnol Bioeng 2012;109:1898–911.
[11] Flanagan LA, Ju YE, Marg B, Osterfield M, Janmey PA. Neurite branching on deformable substrates. Neuroreport 2002;13:2411–5.
[12] Georges PC, Miller WJ, Meaney DF, Sawyer ES, Janmey PA. Matrices with compliance comparable to that of brain tissue select neuronal over glial growth in mixed cortical cultures. Biophys J 2006;90:3012–8.
[13] Moshayedi P, Costa LD, Christ A, Lacour SP, Fawcett J, Guck J, et al. Mechanosensitivity of astrocytes on optimized polyacrylamide gels analyzed by quantitative morphometry. J Phys Condens Matter 2010;22. http://dx.doi.org/10.1088/0953-8984/22/19/194114.

[14] Franze K, Guck J. The biophysics of neuronal growth. Rep Prog Phys 2010;73. http://dx.doi.org/10.1088/0034-4885/73/9/094601.
[15] Franze K. Atomic force microscopy and its contribution to understanding the development of the nervous system. Curr Opin Genet Dev 2011;21:530–7.
[16] Jagielska A, Norman AL, Whyte G, Vliet KJ, Guck J, Franklin RJ. Mechanical environment modulates biological properties of oligodendrocyte progenitor cells. Stem Cells Dev 2012;21:2905–14.
[17] Franze K, Janmey PA, Guck J. Mechanics in neuronal development and repair. Annu Rev Biomed Eng 2013;15:227–51.
[18] Wilby MJ, Muir EM, Fok-Seang J, Gour BJ, Blaschuk OW, Fawcett JW. N-Cadherin inhibits Schwann cell migration on astrocytes. Mol Cell Neurosci 1999;14:66–84.
[19] Irizarry RA, Hobbs B, Collin F, Beazer-Barclay YD, Antonellis KJ, Scherf U, et al. Exploration, normalization, and summaries of high density oligonucleotide array probe level data. Biostatistics 2003;4:249–64.
[20] Binder H, Preibisch S, Berger H. Calibration of microarray gene-expression data. Methods Mol Biol 2010;576:375–407.
[21] Christ AF, Franze K, Gautier H, Moshayedi P, Fawcett J, Franklin RJ, et al. Mechanical difference between white and gray matter in the rat cerebellum measured by scanning force microscopy. J Biomech 2010;43:2986–92.
[22] Lu YB, Franze K, Seifert G, Steinhauser C, Kirchhoff F, Wolburg H, et al. Viscoelastic properties of individual glial cells and neurons in the CNS. Proc Natl Acad Sci U S A 2006;103:17759–64.
[23] Kreutzberg GW. Microglia: a sensor for pathological events in the CNS. Trends Neurosci 1996;19:312–8.
[24] Basu A, Krady JK, Levison SW. Interleukin-1: a master regulator of neuroinflammation. J Neurosci Res 2004;78:151–6.
[25] Goritz C, Dias DO, Tomilin N, Barbacid M, Shupliakov O, Frisen J. A pericyte origin of spinal cord scar tissue. Science 2011;333:238–42.
[26] Georges PC, Hui JJ, Gombos Z, McCormick ME, Wang AY, Uemura M, et al. Increased stiffness of the rat liver precedes matrix deposition: implications for fibrosis. Am J Physiol Gastrointest Liver Physiol 2007;293:G1147–54.
[27] Zhao G, Cui J, Qin Q, Zhang J, Liu L, Deng S, et al. Mechanical stiffness of liver tissues in relation to integrin beta1 expression may influence the development of hepatic cirrhosis and hepatocellular carcinoma. J Surg Oncol 2010;102:482–9.
[28] Glasser SP. On arterial physiology, pathophysiology of vascular compliance, and cardiovascular disease. Heart Dis 2000;2:375–9.
[29] Engler AJ, Sweeney HL, Discher DE, Schwarzbauer JE. Extracellular matrix elasticity directs stem cell differentiation. J Musculoskelet Neuronal Interact 2007;7:335.
[30] Gilmour D, Knaut H, Maischein HM, Nusslein-Volhard C. Towing of sensory axons by their migrating target cells in vivo. Nat Neurosci 2004;7:491–2.
[31] Hardie RC, Franze K. Photomechanical responses in Drosophila photoreceptors. Science 2012;338:260–3.
[32] Blakney AK, Swartzlander MD, Bryant SJ. The effects of substrate stiffness on the in vitro activation of macrophages and in vivo host response to poly(-ethylene glycol)-based hydrogels. J Biomed Mater Res A 2012;100:1375–86.
[33] Buxboim A, Rajagopal K, Brown AE, Discher DE. How deeply cells feel: methods for thin gels. J Phys Condens Matter 2010;22:194116.
[34] Kuo CH, Xian J, Brenton JD, Franze K, Sivaniah E. Complex stiffness gradient substrates for studying mechanotactic cell migration. Adv Mater 2012;24:6059–64.